

AMERICAN UNIVERSITY OF BEIRUT

ASSESSING THE ANTICANCER POTENTIAL OF ONC201
AND ONC206 IMIPRIDONES ON HUMAN PROSTATE
CANCER USING 2D AND 3D CELL MODELS

by
SANA IZZAT HACHEM

A thesis
submitted in partial fulfillment of the requirements
for the degree of Master of Science
to the Department of Anatomy, Cell Biology and Physiological Sciences
of the Faculty of Medicine
at the American University of Beirut

Beirut, Lebanon
August 2023

AMERICAN UNIVERSITY OF BEIRUT

ASSESSING THE ANTICANCER POTENTIAL OF ONC201
AND ONC206 IMIPRIDONES ON HUMAN PROSTATE
CANCER USING 2D AND 3D CELL MODELS

by
SANA IZZAT HACHEM

Approved by:

Signature



Dr. Wassim Abou-Kheir, Associate Professor
Department of Anatomy, Cell Biology & Physiological Sciences

Advisor

Signature



Dr. Assaad Eid, Professor
Department of Anatomy, Cell Biology & Physiological Sciences

Member of Committee

Signature



Dr. Georges Daoud, Associate Professor
Department of Anatomy, Cell Biology & Physiological Sciences

Member of Committee

Signature



Dr. Larry Bodgi, Assistant Professor
Department of Radiation Oncology

Member of Committee

Date of thesis defense: August 28, 2023

ACKNOWLEDGEMENTS

This project wouldn't have been possible without the support of many people.

To the one behind it all, Dr. Wassim Abou-Kheir. From the first class I took with you, I knew I wanted to work in your laboratory, and if I had to go back in time I'd always choose your lab. You were not only a great advisor, but also a friend and my number one support system. Thank you for believing in me during my hard times of self-doubt. Thank you for encouraging me to overcome all technical obstacles towards achieving milestones. Thank you for pushing me to become the best version of myself. You inspired and motivated me to strive for the highest standards. Your exceptional mentorship, continuous guidance and unwavering support made me the researcher I am today. I will be forever grateful to have had the chance to work under your supervision. Your influence will undoubtedly resonate in my academic and professional pursuits, and for that, I am truly grateful and owe you my future success.

I would like to thank Dr. Assaad Eid, Dr. Georges Daoud and Dr. Larry Bodgi for being part of my committee. I really appreciate your time and feedback.

To my mentor Amani, thank you for everything you have done to me. Your mentorship, invaluable help and insightful feedbacks have led me to successfully complete my thesis. I am truly fortunate to have had the opportunity to learn from you.

I have been encouraged, sustained, empowered and tolerated not only by my family, but by the greatest group of friends anyone ever has. To my fellow WAKers, thank you for making my thesis journey enjoyable and unforgettable. I will forever cherish all our memories together. Your presence has been a source of immense joy and strength. Thank you for the laughter that eased the stress, and the countless cups of coffee that kept us going. Thank you for supporting me in countless ways and for being my comfort zone. I am deeply grateful for the bonds we've formed and for the memories we've shared. I love you all!

Finally, I am deeply thankful to my family for their unconditional love, continuous support and encouragements throughout my years of study. Thank you for all the sacrifices you've made, your belief in me and your continuous reassurance. This thesis is a reflection of not only my dedication but also the support system you've provided.

ABSTRACT OF THE THESIS OF

Sana Izzat Hachem

for

Master of Science

Major: Human Morphology

Title: Assessing the Anticancer Potential of ONC201 and ONC206 Imipridones on Human Prostate Cancer Using 2D and 3D Cell Models

Background: Prostate cancer (PC) is the second most commonly diagnosed cancer and the fifth leading cause of cancer-related deaths among men worldwide. Although many therapeutic approaches have been used to manage PC, the disease often develops resistance and progresses into an aggressive and lethal state, known as metastatic castration-resistant prostate cancer (mCRPC). Therefore, defining new targets and elucidating novel therapeutics for treating and managing PC are of utmost priority. Imipridones represent a novel class of anti-cancer compounds that showed promising results in several cancer types. ONC201, the first-in-class clinical imipridone, showed to have anticancer effects in PC. ONC206, an analog derivative of ONC201, possesses enhanced nanomolar potency against several cancers. However, there are no published studies assessing the anti-cancer activity of ONC206 in PC. With ONC206 being more potent than ONC201, it might be able to target the tumors that have acquired therapy resistance mechanisms.

Objective: The aim of this study is to investigate the anti-cancer potential of ONC206, in comparison to ONC201, on human PC using two-dimensional (2D) and three-dimensional (3D) *in vitro* cell models.

Methods: ONC201 and ONC206 drugs were tested on two PC cell lines (DU145 and PC3) using several *in vitro* assays. MTT assay was performed to evaluate the cytotoxic effect of a wide range of concentrations of ONC201 and ONC206 on PC cells. Trypan blue exclusion assay was then used to assess the effect of both drugs on cellular viability. In addition, cell migration ability was investigated using the “wound-healing” scratch assay. Furthermore, the 3D sphere-forming assay was applied to examine the effect of both drugs in targeting the enriched population of PC stem/progenitor cells.

Results: Our MTT data showed that ONC206 exerts a more potent cytotoxic effect on the DU145 and PC3 cell lines compared to ONC201, in a time and dose-dependent manner. These results were confirmed through the trypan-blue viability assay. Similarly, ONC206 displayed a more significant attenuation in the migration ability of PC cells in comparison to ONC201. Importantly, these results were validated in a 3D culture system with the sphere-forming assay, where both imipridones decreased the size and the sphere forming ability of prostatospheres. ONC206 was also more potent than ONC201 in targeting the subpopulation of prostate cancer stem cells.

Conclusion: Imipridones represent a novel therapeutic approach for the management of cancer. Our data shows that ONC206, the analog derivative of ONC201, shows more potent anti-cancer effects on PC cells at nanomolar concentrations, paving the way for new effective therapeutics and better clinical management of PC.

TABLE OF CONTENTS

ACKNOWLEDGEMENTS	1
ABSTRACT.....	2
ILLUSTRATIONS.....	6
ABBREVIATIONS	7
INTRODUCTION	9
1.1. Prostate Cancer	9
1.1.1. Prostate Cancer Epidemiology.....	9
1.1.2. Prostate Gland Anatomy and Function.....	10
1.1.3. Pathogenesis of Prostate Cancer	13
1.1.4. Screening	19
1.1.5. Symptoms and Diagnosis.....	19
1.1.6. Treatments	20
2.1. Imipridones	22
2.1.1. ONC201	23
2.1.2. ONC206.....	27
3.1. Aims of the Study	28
MATERIALS AND METHODS	30
2.1. Cell Culture Conditions	30
2.2. Drug Preparation and Treatment.....	31
2.3. MTT Cell Proliferation Assay	31
2.4. Trypan Blue Exclusion Assay (Viability Assay).....	32

2.5. Wound Healing Assay	33
2.6. Sphere-Formation Assay.....	33
2.7. Statistical Analysis.....	34
RESULTS	36
3.1. ONC201 and ONC206 Imipridones Decreased the Proliferation of DU145 and PC3 cells	36
3.2. ONC201 and ONC206 Imipridones Reduced the Viability of DU145 and PC3 cells	37
3.3. ONC201 and ONC206 Imipridones Attenuated the Migration of DU145 and PC3 cells	38
3.4. ONC201 and ONC206 Imipridones Decreased the Growth of DU145 and PC3 Cell-Derived Spheres	40
DISCUSSION	44
REFERENCES.....	48

ILLUSTRATIONS

Figure

1. GLOBOCAN estimates of incidence and mortality worldwide for prostate cancer in 185 countries.	10
2. Zonal anatomy of the prostate gland.....	11
3. Cellular components of the human prostate gland.....	13
4. The cancer stem cells models.	15
5. Development and progression of prostate cancer in response to androgen deprivation therapy.	17
6. Stages of prostate cancer.....	18
7. Molecular structure of ONC201	24
8. Mechanisms of action of ONC201.	26
9. Molecular structure of ONC206	27
10. Representative images of DU145 and PC3 cell lines.	30
11. ONC201 and ONC206 decrease the proliferation of DU145 and PC3 cell lines in a time and dose-dependent manner.....	37
12. ONC201 and ONC206 reduce the viability of DU145 and PC3 cell lines in a time and dose-dependent manner.	38
13. ONC201 and ONC206 attenuate the migration of DU145 prostate cancer cells.	39
14. ONC201 and ONC206 attenuate the migration of PC3 prostate cancer cells. ...	40
15. ONC201 and ONC206 decrease the sphere-forming unit and size of DU145-derived spheres.	42
16. ONC201 and ONC206 decrease the sphere-forming unit and size of PC3-derived spheres.	43

ABBREVIATIONS

2D: Two-Dimensional

3D: Three-Dimensional

ABCG2: ATP-Binding Cassette G 2

ADT: Androgen Deprivation Therapy

AJCC: American Joint Committee on Cancer

Akt: Protein Kinase B

ALDH1: Aldehyde Dehydrogenase 1

AR: Androgen Receptor

ATF4: Activating Transcription Factor 4

AUA: American Urological Association

BPH: Benign Prostatic Hyperplasia

BT: Brachytherapy

CHOP: C/EBP Homologous Protein

ClpP: Caseinolytic Protease P

CSCs: Cancer Stem Cells

DHT: Dihydrotestosterone

DMSO: Dimethylsulfoxide

DRD2: Dopamine D2 Receptor

EBRT: External Beam Radiotherpay

eIF2- α : Eukaryotic Initiation Factor 2 α

ERK: Extracellular Signal–Regulated Kinase

Foxo3a: Forkhead Box O3a

GPCR: G Protein-Coupled receptor

IARC: International Agency for Research on Cancer

IC50: Half-Maximal Inhibitory Concentration

ISR: Integrated Stress Response

mCRPC: Metastatic Castration-Resistant Prostate Cancer

MTT: [3-(4, 5-dimethylthiazol-2-yl)-2, 5-diphenyltetrazolium

OD: Optical Density

PBS: Phosphate-Buffered Saline

PC: Prostate Cancer

PCSCs: Prostate Cancer Stem Cells

PIN: Prostatic Intraepithelial Neoplasia

PSA: Prostate Specific Antigen

ROS: Reactive Oxygen Species

SEM: Standard Error Mean

SFU: Sphere Formation Unit

TIC10: TRAIL-Inducing Compound 10

TME: Tumor Microenvironment

TNF: Tumor Necrosis Factor

TRAIL: TNF-Related Apoptosis-Inducing Ligand

TRUS: Transrectal Ultrasound

CHAPTER 1

INTRODUCTION

1.1. Prostate Cancer

1.1.1. Prostate Cancer Epidemiology

Cancer is a heterogeneous disease arising due to aberrant multifunctional genomic processes that induce the progressive transformation of normal cells into neoplastic tissues. These tissues abnormally proliferate and invade neighboring cells leading to the formation of malignant tumors [1]. Cancer has become a fatal global health concern that persists to rank as the second leading cause of mortality worldwide accounting for almost 19.3 million new cases and approximately 10 million deaths as reported by the 2020 GLOBOCAN estimates of cancer incidence and mortality issued by the International Agency for Research on Cancer (IARC). These statistics are predicted to exponentially increase by 47% by the year 2040 which calls for the need of global cancer control especially in low- and middle-income countries [2].

Prostate cancer (PC) is the second most frequently diagnosed cancer among men worldwide with around 1.4 million new cases (14.1% of all cancers) and the fifth leading cause of cancer-related deaths with 375,304 deaths (6.8% of all cancers) as estimated by GLOBOCAN 2020 [2] (Figure 1). These numbers imply that about 1 in 8 men are diagnosed with PC, which reflects the high global incidence rate of this disease. In Lebanon, PC is the most commonly occurring cancer among men [3]. Men of age 50 years tend to have higher risks of developing PC [2]. The well-established risk factors of PC include age, family history, ethnicity, lifestyle and dietary patterns [4]. Thus,

screening and early diagnosis remain the main strategies to manage and control the increasing burden of PC [4].

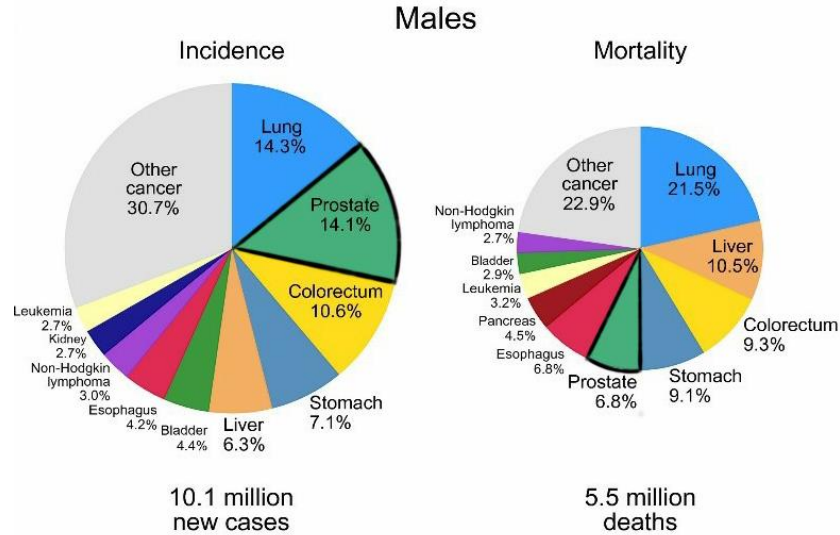


Figure 1. GLOBOCAN estimates of incidence and mortality worldwide for prostate cancer in 185 countries. Distribution of incidence and mortality for the top 10 most common cancers in 2020 in men according to global cancer statistics 2020 [Adapted and modified from [2]].

1.1.2. Prostate Gland Anatomy and Function

The prostate is the largest accessory exocrine gland of the male reproductive system. It is an androgen-sensitive gland whose primary function is to produce a slightly alkaline fluid (pH~6) that contains zinc, citric acid, proteolytic enzymes and antimicrobial proteins [5]. These secretions provide nourishment and motility to the sperms, hence promoting male fertility [6]. The prostatic fluid makes up 30% of the semen and contributes to its milky appearance [7]. The prostate gland is located in the retroperitoneal space in men. It has an inverted pyramid-like shape with its base surrounding the bladder and its apex wrapping the urethral membrane at the superior part of the urogenital diaphragm [5]. The normal adult prostate is about the size of a chestnut and weighs 15 to 20 g [8, 9]. In the 20th century, McNeal and his colleagues

defined the prostate gland in terms of 4 distinct anatomical zones, each derived from different embryonic origins [10] (Figure 2):

- The peripheral zone extends from the apex to the base, it surrounds the distal urethra and makes up 70% of the glandular prostatic tissue. This zone is the main site of inflammation and the most susceptible to carcinogenesis.
- The central zone constitutes the base of the gland and accounts for 25% of the total glandular prostate. It has a conical shape and surrounds the ejaculatory ducts. This zone is resistant to both cancer and inflammation.
- The transition zone or also termed as pre-prostatic region only constitutes 5% of the glandular prostate. It's the exclusive site of benign prostatic hyperplasia (BPH) but might also be prone to carcinoma.
- The anterior fibromuscular stroma or pre-urethral zone is the most anterior part of the prostate and completely lacks any glandular tissue.

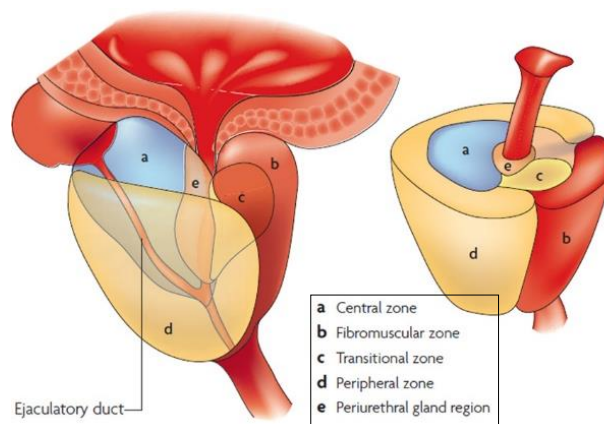


Figure 2. Zonal anatomy of the prostate gland. The prostate gland is divided into an anterior fibromuscular stroma and three glandular zones: the peripheral (70% of the glandular tissue), the central zone (20% of the glandular tissue) and the transition zone (5% of the glandular tissue) [adopted and modified from [11]].

At the cellular level, the prostate gland is histologically heterogeneous. It's mainly composed of epithelial and stromal compartments. The fibromuscular stroma is

mainly involved in the regulation of the microenvironment of epithelial cells and in the maintenance of its homeostasis. It consists of the extracellular matrix, smooth muscles, immune cells and provides vasculature and innervation to the gland [12]. Meanwhile, the epithelial compartment performs the glandular functions of the prostate [6]. It's stratified into 3 cell types: secretory columnar epithelial cells, cuboidal basal epithelial cells and neuroendocrine cells (Figure 3).

The secretory cells line the acinar lumen and are responsible for the synthesis of prostatic proteins, mainly prostate specific antigen (PSA) and prostate specific phosphatases that will be secreted into the seminal fluid. The structural and functional state of these cells is under the influence of androgenic stimulation. As such, the absence of androgen induce them to undergo apoptosis leading to prostate gland involution [13].

The neuroendocrine cells are sparse cells located on the basal lamina corresponding to only 1% of the total prostatic epithelium [14]. Neuroendocrine cells lack androgen receptors (ARs) and PSA expressions [15]. They secrete hormones, neuropeptides and cytokines that play a critical role in the growth of the gland and the regulation of its exocrine secretory function [16].

The basal cells are present on the lining of the basement membrane and lack AR expression. Instead, they express stemness markers such as $\alpha_2\beta_1$ integrin, CD44 and CD133 in addition to the typical basal markers CK5 and CK14 [17, 18]. Therefore, these cells are considered to be the main multipotent stem cells that can differentiate into all epithelial cell types of the prostate gland [18-20]. The existence of basal stem cells was established based on *in vivo* studies in which castration of male rats resulted in the apoptosis of differentiated secretory epithelial cells, while the basal cells were

spared. Interestingly, upon androgen exposure, the gland was fully reconstituted [21]. Together, these findings indicate that the androgen-independent basal stem cells can give rise to androgen-sensitive progenitor cells. Upon androgen stimulation the androgen-sensitive cells differentiate into an androgen-dependent phenotype and can therefore reconstitute the prostatic epithelium [22].

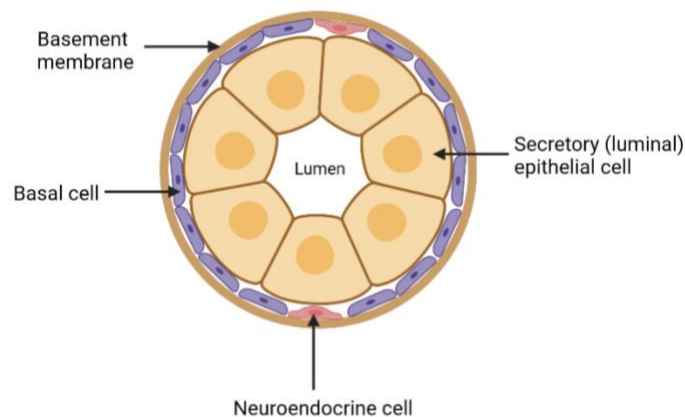


Figure 3. Cellular components of the human prostate gland. Secretory epithelial cells face the acinar lumen of the gland and synthesize the proteins constituting the prostatic fluid. Rare neuroendocrine cells line the basement membrane and support the secretory cells. Basal cells constitute the stem cells of gland. Created with BioRender.com

1.1.3. Pathogenesis of Prostate Cancer

The phenotypic heterogeneity of solid tumors is a major contributor to cancer hallmarks [23]. PC is labeled as a model for inter/intra tumor heterogeneity at the clinical, histological and molecular levels [24]. Indeed, PC harbors phenotypically distinct cell types including cancerous epithelial cells as well as non-epithelial stromal cells. Oncogenic mutations affecting specific cell types eventually lead to tumors of different molecular and histomorphological properties [25]. Genetic and epigenetic alterations can induce the transformation of normal prostatic epithelial basal cells into malignant ones. Thus, the normal prostate stem cells are mutated into tumor-initiating

cells or PC stem cells (PCSCs) that can now drive tumor growth and progression [26]. Other mutations targeting rare luminal epithelial stem cells can also trigger the initiation of PC [27].

1.1.3.1. Cancer stem cells

Tumor heterogeneity can be explained in terms of the cancer stem cells (CSCs) model (Figure 4). This model speculates that a small subpopulation of CSCs, also termed as tumor-initiating cells, is situated at the apex of the hierarchical cellular organization. In fact, CSCs are analogous to normal multipotent stem cells and possess a panel of stemness characteristics. The dysregulated stemness pathways allow CSCs to self-renew and differentiate into progenitor cells with less differentiation ability. These cells expand extensively and eventually mature into fully differentiated heterogeneous malignant cell populations that can reconstitute the tumor bulk [28]. As such, the CSCs niche can initiate cancer propagation and continuously sustain its tumorigenesis [29]. Importantly, CSCs can influence neighboring cells to provide a suitable tumor microenvironment (TME) that supports tumor growth [30, 31]. The properties associated with CSCs impose them as important contributors to cancer metastasis, relapse and therapy resistance [31, 32]. CSCs exhibit high plasticity and can be generated by two mechanisms. The first one is the result of accumulating oncogenic mutations that induce the transformation of normal stem cells into CSCs [33]. The second one relies on a de-differentiation process in which mature fully differentiated cells undergo epithelial to mesenchymal transition and acquire stemness properties [34].

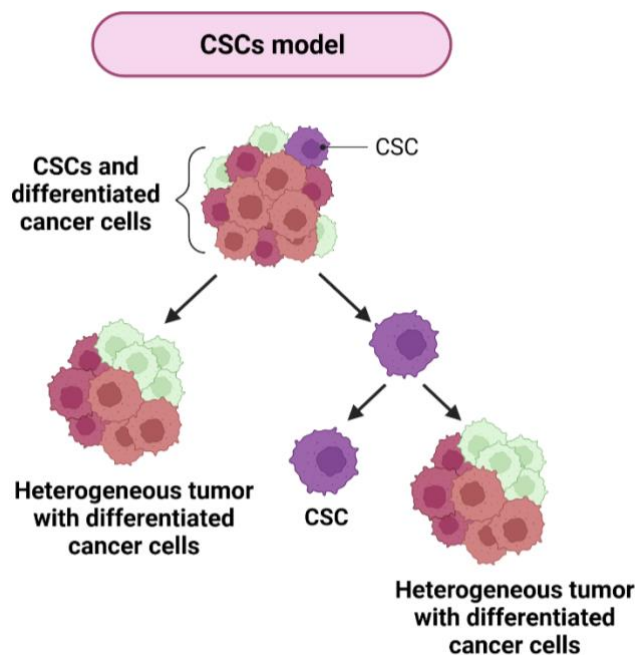


Figure 4. The cancer stem cells models. The CSCs model suggests that cancer is driven by tumor-initiating cells possessing self-renewal ability known as CSCs. CSCs undergo symmetrical and asymmetrical divisions to give rise to differentiated cancer cells as well as new CSCs. The newly generated CSCs can maintain their stemness ability allowing the tumor to continuously proliferate and recapitulate the heterogeneous phenotype. CSC: cancer stem cell. Created with BioRender.com

1.1.3.2. Prostate cancer stem cells

PCSCs were first identified by Collin et al. in 2005 based on the normal prostate stem cells surface markers CD44, CD133 and integrin $\alpha 2\beta 1$ [35]. These cells were isolated from human biopsies of patients with primary and metastatic PC. The isolated PCSCs exhibited high self-renewal potential. Indeed, the selected cells had a basal phenotype (expressing CK14 and CK8 and lacking AR) and showed high proliferative ability *in vitro*. In addition, the cells were able to differentiate into a PSA⁺/AR⁺ luminal secretory phenotype, reflecting their ability to recapitulate the original tumor cells *in situ*. Notably, these cells possessed high invasive properties and could survive under anchorage-independent conditions [35]. Another study showed that cells isolated from

primary prostate tumors having a CD133⁺/CD44⁺ phenotype were able to fully reconstitute the parental human tumor from which they were derived when transplanted into immunocompromised mice [36]. Due to the significant role that CSCs play in PC initiation and progression, numerous efforts have been undertaken to detect and isolate them from the tumor bulk using the specific markers they exhibit. These markers mainly include CD44, CD133, CD49f, CD117, EpCAM, Aldehyde dehydrogenase (ALDH1a) and ATP-Binding Cassette (ABCG2) among others [37].

In addition to their role in cancer initiation and progression, PCSCs are also implicated in therapy resistance. A compelling body of evidence suggests that these slowly dividing and quiescent cells can resist conventional treatments including radiation, chemotherapy and hormonal therapy [38-41].

1.1.3.3. Progression of prostate cancer

The oncogenic abnormalities mediating PC lead to morphological and histological changes that start with pre-cancerous lesions designated as prostatic intraepithelial neoplasia (PIN) and correspond to low grade prostate tumors. PIN involves the increase in the proliferation of luminal secretory cells and the decrease in the number of basal cells. As PIN advances, it transforms into invasive adenocarcinoma characterized by a luminal AR⁺/PSA⁺ phenotype and undergoes complete loss of the basal cells along with the basement membrane. This progression results in different tumor grades, ranging from less aggressive to more aggressive forms of PC, ultimately leading to metastasis [42]. When subjected to conventional androgen deprivation therapy (ADT), cells expressing a positive AR profile are targeted while cells lacking the AR phenotype will activate cell survival pathways [42]. The resulting tumor

phenotype switches to AR⁻/PSA⁻ PCSCs cells that will predominate the tumor bulk [43]. These cells will eventually promote tumor re-growth and recapitulate the malignant features. At this advanced stage, PC is known as metastatic castration-resistant PC (mCRPC) as it is insensitive to androgen signaling. This aggressive form constitutes a high grade tumor that manifests high self-renewal and differentiation abilities (Figure 5). Accordingly, PCSCs will drive tumor progression and invasion into neighboring tissues including the lymph nodes and the bones [44]. mCRPC is often lethal as the disease also metastasizes into vital organs such as the liver and the lungs [42].

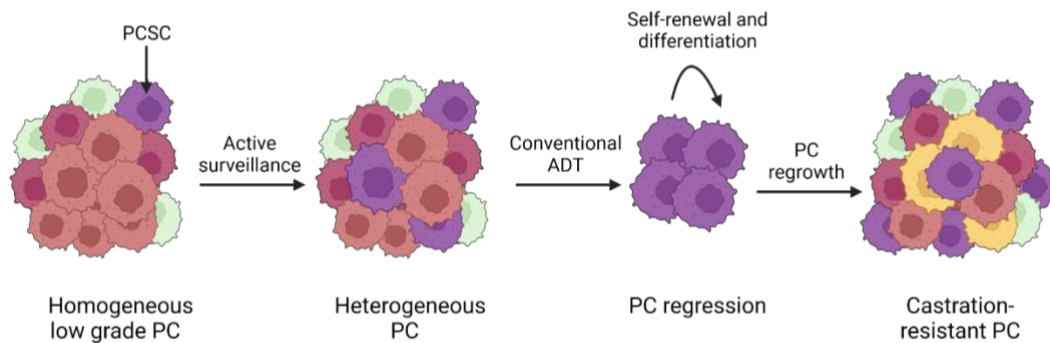


Figure 5. Development and progression of prostate cancer in response to androgen deprivation therapy. At early stages of prostate cancer, the tumor consists of androgen-dependent cancerous cells. These cells are targeted by androgen deprivation therapy, which leads to prostate cancer regression. PCSCs that do not express androgen receptors activate cell survival mechanisms and can now self-renew and differentiate to recapitulate the heterogeneous tumor. This tumor is now insensitive to androgen deprivation and has a more aggressive phenotype corresponding to metastatic castration-resistant prostate cancer. PC: prostate cancer, PCSC: prostate cancer stem cell, ADT: androgen deprivation therapy. Created with BioRender.com

1.1.3.4. Clinical and pathological stages of prostate cancer

At the clinical level, PC stages can be classified by the tumor, node, and metastasis (TNM) system elaborated by the American Joint Committee on Cancer (AJCC). The T category assesses the size and the location of PC and corresponds to a primary localized tumor. The N category refers to the invasion of PC to lymphoid tissues. The M category reflects the metastasis of PC into secondary distant organs [45].

TNM staging is followed by a pathological grading system known as Gleason score in order to assess the aggressiveness of the tumor. The pathologist investigates morphological and histological aspects of PC cells in two distinct areas and assigns a score ranging from 3 to 5. The scores are added up to reach an overall score between 6 and 10. At score 6 or lower, PC cells are similar to normal prostate cells and correspond to a low-grade tumor; at score 7 PC cells refer to a medium-grade tumor; higher scores indicate a high-grade tumor with increased PC growth and abnormal morphology [46]. By combining the results of TNM staging and Gleason scores along with PSA level, PC staging can be determined. Stage I implicates that the tumor is still confined within the gland. At stage II the cancer has still not spread but cancerous cells are more abnormal and prevalent within the gland. Advanced stage III describes the progression of PC into neighboring organs. Finally, stage IV indicates that PC metastasized into distant body parts [45] (Figure 6).

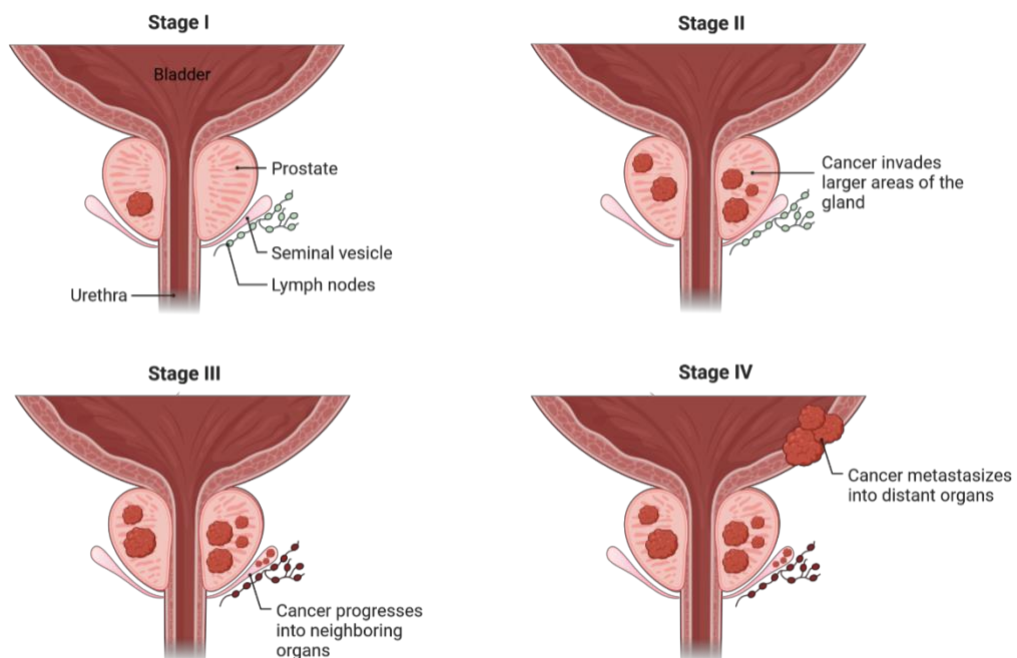


Figure 6. Stages of prostate cancer. At stage I, the tumor is initiated in a confined area of the gland. At stage II, cancerous cells proliferate to invade adjacent prostatic tissue. At stage III, prostate cancer progresses into neighboring organs such as the lymph nodes and seminal vesicles. At stage IV, prostate cancer metastasizes into distant organs (For instance, the bladder). Created with BioRender.com

1.1.4. Screening

At early stages of the disease, PC is often asymptomatic. By the time symptoms become prevalent, PC would have reached advanced stages and might become difficult to treat. Thus, the American Urological Association (AUA) recommends screening to asymptomatic average risk men starting the age of 55 years [47]. However, PC screening is a very controversial topic in urology due to the unreliable techniques currently being employed. Indeed, PSA blood level, a widely used screening test, can often be misleading because PSA levels may rise not only due to cancer but also due to BPH and other prostatic inflammatory diseases [48]. In other terms, PSA test can result in over-diagnosis and over-treatment which ultimately subject the patients to complications associated with biopsies [49, 50]. Another commonly used screening modality is the digital rectal examination (DRE). This test aims to assess abnormal changes in the size and consistency of the prostate gland. However, this test lacks specificity because it fails to detect early-stage PC and can also result in over-diagnosis [51]. Thus, novel screening tools should be used in order to provide accurate detection of PC and limit the complications associated with its progression. These tools mostly include radiological imaging (mpMRI), serum biomarkers (4Kscore, PHI) and urine biomarkers (PCA3, HOXC6/DLX1) or a combination of several screening tools [52].

1.1.5. Symptoms and Diagnosis

Although there are no ultimately reliable PC symptoms, some clinical signs might indicate the presence of the disease. Since most prostate carcinoma arise in the peripheral zone of the gland surrounding the urethra, urinary symptoms such as nocturia, frequent urination, hematuria and dysuria might correlate with early PC.

Additionally, sexual dysfunction can be linked to PC. With the progression of the tumor, advanced PC symptoms generally translate as fatigue, pain in the bones, paralysis and renal failure [53]. The standard diagnosis of PC mainly relies on transrectal ultrasound (TRUS) or MRI guided biopsies in which the urologist extracts around 12 core samples from different areas of the gland that will be tested for pathology [54].

1.1.6. Treatments

Once diagnosis has been confirmed, several lines of treatment can be adopted. The treatment strategies depend on the stage of the disease (PSA levels, Gleason score), pathohistological aspects of PC cells and the degree of cancer progression.

1.1.6.1. Active surveillance

Since PC tends to grow slowly and is often asymptomatic, some patients don't need any type of medical interventions. Instead, active surveillance is recommended in order to prevent the complications associated with overt-treatment while ensuring the same clinical outcomes as in patients undergoing therapy. This involves ritual screening including DRE and PSA blood levels every 6 months as well as imaging tests to monitor the status of PC progression [55].

1.1.6.2. Surgery

Radical prostatectomy is recommended for men with intermediate- and high-risk PC. This approach aims to suppress the metastasis of PC cells by the surgical removal

of the gland along with the surrounding lymph nodes. This treatment strategy is not considered as monotherapy since it is often followed by radiation therapy [56].

1.1.6.3. Radiotherapy

The two main treatment modalities of radiotherapy include external beam radiotherapy (EBRT) and brachytherapy (BT). When PC is strictly confined within the gland, BT or internal radiation therapy is often used. It relies on the insertion of radioactive seeds within the prostate. The seeds emanate radiation just around the affected area and spare the surrounding normal cells [57]. In EBRT, the radiation beams (proton or photon beams) are directed towards the cancerous cells while minimizing their toxic effect on normal cells [58]. For patients with intermediate or high-risk PC, EBRT is often combined with other lines of treatments including radical prostatectomy and ADT [59].

1.1.6.4. Hormonal therapy

As mentioned previously, the prostate gland is an androgen-dependent organ that requires androgens, typically testosterone and dihydrotestosterone (DHT) for growth and development [60]. Thus, the first front-line treatment in case of advanced PC is ADT. ADT lowers androgen levels either through surgical castration (removal of testicles), or by medical castration (inhibition of AR signaling pathway). Blocking the AR pathway can be achieved through two main approaches. The first one relies on the use of non-steroidal AR antagonists (for example enzalutamide, apalutamide, and darolutamide) to inhibit the binding of testosterone and DHT to AR [61]. The second one works on blocking the conversion of steroids precursors to androgens by

suppressing the hypothalamic-pituitary-gonadal axis (for example diethylstilbestrol) as well as the hypothalamic-pituitary-adrenal axis (for example abiraterone) [61, 62].

1.1.6.5. Immunotherapy

Immunotherapy can be used in patients with mCRPC who have not undergone chemotherapy. It relies on the use of vaccines that trigger the patient's immune system to attack and destroy cancerous cells. This is done through the modification of the host's immune cells to be able to recognize PC cells expressing AR, and PSA as antigenic targets [63]. Sipuleucel-T and pembrolizumab are FDA-approved therapeutic vaccines that act as immune-activator and programmed cell death of regulatory T-cells inhibitors respectively [63].

1.1.6.6. Chemotherapy

Chemotherapy is administered to patients who fail to respond to ADT when PC advances into an androgen-independent stage [64]. Docetaxel, the first-line chemotherapeutic, showed to have survival advantage in patients with mCRPC and metastatic castration-sensitive PC. When combined with prednisone, the cytotoxic chemotherapeutic effect of docetaxel increases significantly [65]. The second-line chemotherapeutic agent is cabazitaxel. However, it fails to achieve greater efficacy in chemotherapy-naïve patients [66].

2.1. Imipridones

Standard treatments for PC fail to achieve satisfactory results because cancer cells eventually develop resistance. Therefore, novel disease-targeted therapies are

needed to overcome the resistance associated with conventional treatments. Imipridones represent a novel class of anti-cancer compounds that present promising results in targeting several resistance mechanisms including the self-renewal and differentiation pathways of CSCs [67].

2.1.1. *ONC201*

2.1.1.1. Origin and structure of ONC201

ONC201, is the first in-class clinical drug of the new imipridone family of anti-cancer compounds. It was first identified in a phenotypic cell-based screening of colorectal cancer cells unlike most anti-cancer agents that are recognized using target-structure based screening. Indeed, ONC201 was discovered as a p53-independent inducer of the tumor necrosis factor (TNF)-related apoptosis-inducing ligand (TRAIL) pathway. Accordingly, ONC201 was initially referred to as TRAIL-inducing compound 10 (TIC10) [68]. TRAIL is a tumor suppressor protein expressed on immune cells that induces apoptosis of adjacent cancerous cells, while sparing normal cells [69]. Thus, the first purpose of ONC201 was to be used as a TRAIL-based therapy due to its natural anti-cancer pro-apoptotic activity [68].

ONC201 or 7-benzyl-4-(2-methylbenzyl)-1,2,6,7,8,9- hexahydroimidazo [1,2-a]pyrido [3,4-e]pyrimidin-5(1H)-one, is a small molecule characterized by a unique heterocyclic pharmacophore core (Figure 7). The imidazo pyridopyrimidone core, also known as the imipridones core, confers many chemical properties to ONC201 allowing it to be a potent drug. These properties include its ease of synthesis, high stability, high aqueous solubility, oral bioavailability, passive penetration to the blood-brain barrier and its high safety profile of decreased cytotoxicity to normal cells [68, 70].

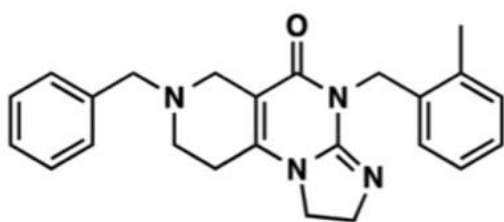


Figure 7. Molecular structure of ONC201

2.1.1.2. Mechanisms of action of ONC201

ONC201 was shown to target four main carcinogenesis pathways (Figure 8). First, it can induce tumor apoptosis via TRAIL activation. TRAIL is positively regulated by the tumor suppressor Forkhead box O3a (Foxo3a) transcription factor. Foxo3a binds to the promotor region of TRAIL and activates it. In tumor cells, the phosphorylation of Foxo3a by pro-survival kinases such as extracellular signal-regulated kinase (ERK) and protein kinase B (Akt) inhibits it from activating TRAIL [69, 71]. However, upon ONC201 administration, ERK and Akt pathways are inactivated which dephosphorylates Foxo3a allowing it to translocate to the nucleus in order to bind to TRAIL's promotor. Once activated, TRAIL can bind to the death receptors DR4 and DR5 expressed on cancer cells, thus inducing tumor-specific apoptosis [68].

In solid tumors, ONC201 also operates under the activating transcription factor (ATF4)/ C/EBP Homologous Protein (CHOP) axis that also activates apoptosis of cancer cells [72]. This is done through an integrated stress response (ISR) in which ONC201 leads to the phosphorylation of eukaryotic initiation factor 2 (eIF2- α) that will increase the translation of the transcription factor ATF4. In turn, ATF4 activates CHOP, another transcription factor that regulates pro-apoptotic genes such as DR5 leading to cancer cells death via a TRAIL-independent pathway [73, 74].

As ONC201 was identified based on its activation of the TRAIL pathway, several studies aimed at pointing out its molecular targets. Interestingly, ONC201 was shown to possess selective competitive and non-competitive antagonism to dopamine receptor 2 (DRD2) and DRD3 with weaker activity on DRD4 [75]. These receptors belong to the group of D2-like receptors of the G protein-coupled receptors (GPCRs) family. DRD2 is overexpressed in several malignancies including lungs, prostate, colon and breast [67]. While the mechanism of action in which DRD2 impact carcinogenesis is not well understood, it's suggested that it might be involved in proliferation and metastasis [76]. Thus, antagonizing DRD2 provides promising anti-cancer effects.

Another mechanism of action associated with ONC201 activity is its direct activation of the mitochondrial serine caseinolytic protease P (ClpP) via non-covalent allosteric interactions [67]. Treatment with ONC201 results in increased proteolytic activity of ClpP which subsequently enhances the degradation of electron transport chain subunits. These alterations cause mitochondrial dysfunction eventually leading to cancer cell death [77]. Interestingly, ClpP can initiate the ISR by upregulating the ATF4/CHOP pathway which ultimately results in the apoptosis of cancer cells [77, 78].

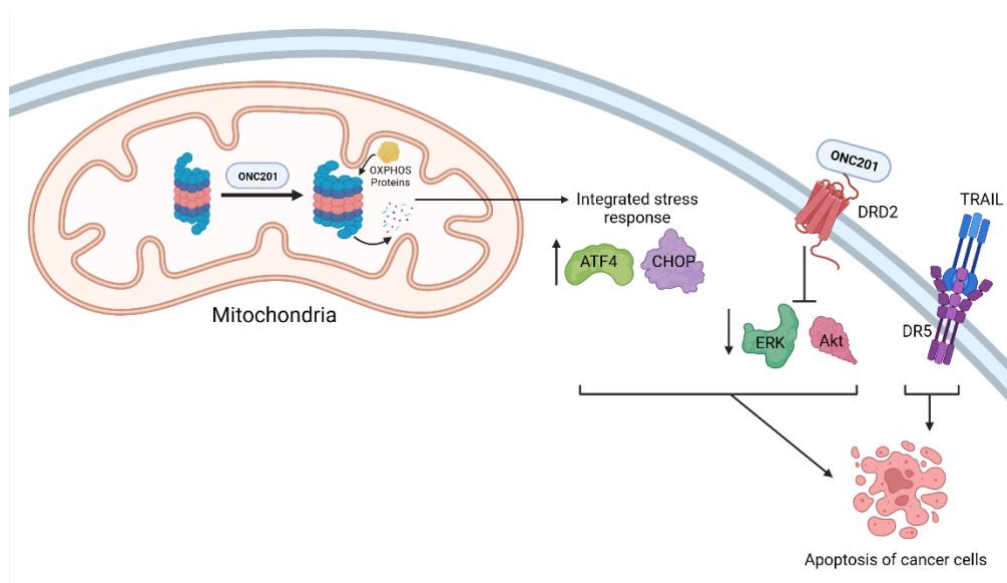


Figure 8. Mechanisms of action of ONC201. ONC201 activates the TRAIL pathway involved in cancer cells apoptosis. It's a DRD2 antagonist and ClpP agonist that induces ISR which ultimately lead to apoptosis of cancerous cells. TRAIL: TNF- related apoptosis-inducing ligand; ISR: integrated stress response; DRD2: dopamine receptor 2; ClpP: caseinolytic protease P. ERK: extracellular signal-regulated kinase; Akt: protein kinase B; ATF4: activating transcription factor; CHOP: C/EBP Homologous Protein. Created with BioRender.com

2.1.1.3. Anti-cancer activity of ONC201 in prostate cancer

ONC201 showed promising anti-cancer effects in several cancers. It is currently in phase II clinical trials for many types of cancers including breast cancer, colorectal cancer, serous endometrial cancer, and ovarian cancer [67].

As for PC, several *in vitro* studies showed that ONC201 is a potent anti-cancer agent. In PC, DRD2 is overexpressed in tumor samples and is implicated in PC progression [79]. ONC201 was shown to exert pro-apoptotic and anti-proliferative effects on five PC cell lines while not affecting normal prostate cells. It was also able to reduce PSA levels by inhibiting the AR pathway. When combined with conventional chemotherapeutics, ONC201 led to a potent synergic effect [80]. Additionally, ONC201 was found to induce PC cells apoptosis via the TRAIL-signaling pathway [81].

Moreover, ONC201 caused PC cells death by activating the ISR in an ATF4/CHOP-dependent manner [82]. Importantly, it was reported that ONC201 can alter the Wnt signaling pathway and downregulate PCSCs markers (such as ALDH1a), leading to a decrease in the self-renewal of PC cell lines [83]. These results were validated *in vitro* and *in vivo* through the sphere formation assay and subcutaneous PC xenografts in mice, indicating that ONC201 can target the subpopulation of PCSCs [80, 83].

ONC201 is currently in phase I clinical trials where it was shown to be biologically active and was able to rapidly reduce the primary prostate tumor as well as metastatic bone lesions [84, 85].

2.1.2. ONC206

2.1.2.1. Structure of ONC206

ONC206 is an imirpidone analog of ONC201 but with enhanced nanomolar potency [86]. ONC206 was derived from changes to the chemical structure of the imidazo pyridopyrimidone pharmacophore of ONC201. This was achieved through the replacement of the R1 group with the fluoride substituent Difluorobenzyl resulting in the more potent ONC206 compound [87] (Figure 9).

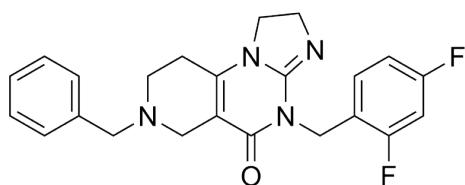


Figure 9. Molecular structure of ONC206

2.1.2.2. Anti-cancer activity of ONC206

ONC206 appears to operate through similar mechanisms of action as its predecessor ONC201. Indeed, nanomolar ONC206 concentrations inhibited cancer cell proliferation and migration by antagonizing DRD2 receptors and activating the ISR pathway in serous endometrial cancer cell lines [86]. A study by El-Soussi *et al.* [88] demonstrated that ONC206 exerts accentuated anti-tumor effect as compared to ONC201 in neuroblastoma cell lines. ONC206 significantly decreased proliferation, viability, and attenuated the migration and invasion potentials of neuroblastoma cells. Interestingly, it was able to target the CSCs subpopulation by decreasing the tumorsphere formation potential of the cells [88]. In the study of Monzer *et al.* ONC206 was shown to inhibit the main carcinogenic processes of colorectal cancer with higher potency than ONC201. Importantly, it was also able to alter self-renewal pathways of colorectal CSCs that are implicated in therapy resistance [89].

ONC206 has not been tested on PC yet. However, with its nanomolar potency, unique bio-distribution and increased non-competitive DRD2 antagonism with respect to ONC201, it could potentially target PC tumors that have acquired resistance mechanisms against conventional treatments.

3.1. Aims of the Study

Although many therapeutic advances have been made to manage PC, this disease often develops drug resistance and progresses into a lethal stage. Therefore, improved cancer-targeted approaches are needed to achieve better clinical outcomes in patients suffering from PC. ONC201 and ONC206 imipridones have shown promising results in various cancers. With ONC206 being more potent than ONC201, it might be

able to target prostate tumors that have acquired therapy resistance. Therefore, the aim of this study is to investigate the anti-cancer potential of ONC206, in comparison to ONC201, on human PC cell lines. This study will assess the cytotoxic effects of both drugs on the proliferation, viability and migration ability using two-dimensional (2D) *in vitro* cell models. Additionally, it will evaluate the therapeutic effect of both imipridones in targeting the enriched subpopulation of PCSCs using a three-dimensional (3D) technique.

CHAPTER 2

MATERIALS AND METHODS

2.1. Cell Culture Conditions

The human PC cell lines DU145 and PC3 previously purchased from the American Type Culture Collection (ATCC; Manassas, VA, USA) were available in our laboratory. DU145 and PC3 are epithelial cells extracted from the brain and the bones of patients with metastatic PC, respectively (Figure 10). The cells were cultured and maintained in RPMI-1640 medium (Sigma-Aldrich) supplemented with 10% heat-inactivated fetal bovine serum (FBS; Sigma- Aldrich), 1 μ g/ml penicillin/streptomycin (Sigma-Aldrich), 5 μ g/ml plasmocin/prophylactic (InvivoGen), 1% non-essential amino acids (Sigma, USA), and 1% sodium pyruvate (Sigma, USA). The cells were incubated in a 37 °C humidified atmosphere of 5% CO₂ and 95% air to reach 80% confluence. The media was replenished every 48 hours and cells were passaged every two to three days when reaching 80% confluency of the flask. All cells were mycoplasma free.

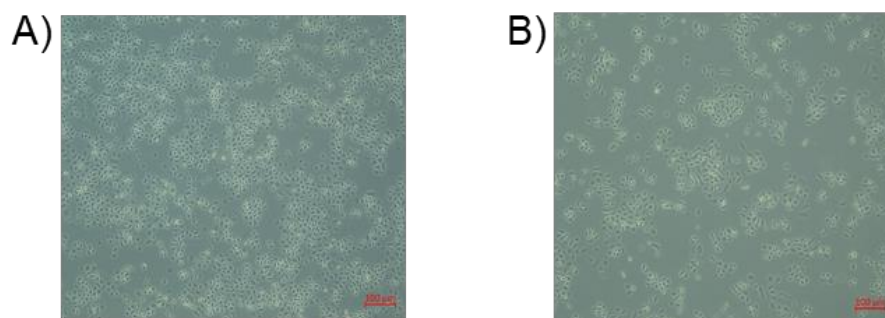


Figure 10. Representative images of DU145 and PC3 cell lines. A) DU145 cells extracted from the brain of patients with metastatic prostate cancer. B) PC3 cells extracted from the bones of patients with metastatic prostate cancer.

2.2. Drug Preparation and Treatment

ONC201 and ONC206 drugs were provided by our collaborator Oncoceutics Inc. (Philadelphia, PA, USA) and were both reconstituted in pure dimethylsulfoxide (DMSO; Sigma-Aldrich), as per manufacturer's instructions. Both drugs were aliquoted in stock solutions of 20 mM and were stored at -20 °C. The stock solutions were then dissolved in cell culture medium to obtain daughter solutions of different concentrations such that the percentage of DMSO on cells was less than 0.1%.

2.3. MTT Cell Proliferation Assay

The anti-proliferative effect of ONC201 and ONC206 was assessed using the MTT ([3-(4, 5-dimethylthiazol-2-yl)-2, 5-diphenyltetrazolium bromide]) (Sigma-Aldrich) assay according to the manufacturer's instructions. This assay relies on the ability of metabolically active cells to reduce the yellow tetrazolium MTT salt into purple formazan crystals via mitochondrial NAD(P)H-dependent oxidoreductase enzymes. The higher the activity of the mitochondrial enzymes, the greater the amount of formazan dye formed, which reflects the number of viable metabolically active cells. Thus, this assay provides an estimation of cellular proliferation. DU145 and PC3 cells were seeded in triplicates in 100 μ L complete media in 96-well plates at a density of 5×10^3 cells/well and incubated overnight. The following day, the sub-confluent cells were treated with several concentrations of ONC201 and ONC206 (0.1, 0.5, 1, 5 and 10 μ M), while the control wells contained growth media and the vehicle consisted of 0.1% pure DMSO corresponding to the highest drug concentration. The cells were then incubated for 24, 48 and 72 hours. For each time point, the old media containing treatment was discarded, 100 μ L of fresh media was added and 10 μ L of 5 mg/mL MTT

reagent (dissolved in 1X phosphate-buffered saline (PBS)) was added to each well and the plate was incubated at 37 °C for 3 hours. After incubation, the reagent was removed and 100 µL of absolute isopropanol (Sigma-Aldrich) was used to solubilize the formazan crystals. The plate was covered by foil and incubated for 1 hour at room temperature. Finally, the reduced MTT optical density (OD) was measured at 595 nm by an ELISA reader (Multiskan Ex). The blank well was used for the baseline zero and the percentage of cell proliferation with respect to control was determined for each drug dose. The data are derived from the mean of triplicate wells of three independent experiments

2.4. Trypan Blue Exclusion Assay (Viability Assay)

The trypan blue viability assay was used to determine the cytotoxic effect of ONC201 and ONC206. In this assay, trypan blue is used as an exclusion dye to discriminate between viable and dead cells. Live cells have intact cell membranes that prevent the dye from penetrating the cytoplasm and appear bright white, while dead cells lose the integrity of their plasma membrane allowing the dye to stain the cells in dark blue. DU145 and PC3 cells were seeded in duplicates in 500 µL complete growth media in 24-well plates at a density of 35×10^3 cells/well and incubated overnight. The next day, the old media was replaced with new complete growth media, vehicle and different ONC201 and ONC206 concentrations (0.5, 1 and 5 µM) and cells were incubated for 24, 48 and 72 hours. For each time point, supernatants containing the dead cells were collected, and the attached live cells were trypsinized, harvested and added to the supernatant. After centrifugation, the cell pellet was re-suspended with 1 mL media. For each condition, 50 µL of cell suspension was mixed with 50 µL of trypan blue. 10 µL of

this mixture was added to the counting chamber of the Neubauer-improved Hemocytometer and visualized under an inverted optical microscope. Viable cells were counted in four quadrants of the two chambers of the hemocytometer and the average was calculated. The percentage of cell viability with respect to control was determined for each drug dose. The data are derived from the mean of duplicate wells of three independent experiments.

2.5. Wound Healing Assay

The wound healing or scratch assay was used to assess the effect of ONC201 and ONC206 on the collective cell migration potential of DU145 and PC3 cells. The cells were seeded in duplicates in 500 μ L complete growth media in 24-well plates with a density of 14×10^4 cells/well and incubated to reach a monolayer of 85-90% confluency. The cells were treated with 10 μ g/mL mitomycin C (Sigma) and incubated for 10 minutes to block cellular proliferation. Using a sterile 200 μ L tip, a scratch (wound) was made. The scraped cells, where the wound was performed, were washed two times with PBS. The remaining cells were then cultured with growth media, vehicle, and drug concentrations of 5 μ M ONC201 and 0.5 μ M ONC206. Images were acquired using bright-field microscopy directly after inducing the scratch (0h), 24h and 48h post-treatment to compare the difference in the wound width. The wound width was measured and expressed as percentage of the relative width for each condition.

2.6. Sphere-Formation Assay

The sphere formation assay was performed to investigate the ability of ONC201 and ONC206 in targeting the highly enriched self-renewing PCSCs pool residing within

the DU145 and PC3 cell lines. This assay was performed according to the protocol previously established by our laboratory [90]. 1000 single cells were suspended in cold Matrigel™/serum-free medium (1:1 dilution) in a total volume of 10 µL. Cells were seeded in duplicates in a circular motion around the rim of the wells of a 96-wells plate. The matrigel was then allowed to solidify for 45 minutes in the incubator at 37 °C. Afterwards, 100 µL of several concentrations of ONC201 and ONC206 drugs diluted in RPMI media with 1% FBS was gently added to the middle of each well. Spheres were replenished with warm media every other day as per the original seeding. After 10-14 days, prostaspheres were counted and bright field images were acquired using Axiovert microscope from Zeiss at 10× magnification. Images were analyzed by Carl Zeiss Zen 2012 image software to determine sphere sizes. Sphere-formation unit (SFU) was calculated as follows:

$$SFU = \frac{\text{Number of spheres formed}}{\text{Number of cells originally plated}} \times 100$$

Results were represented as percentage of the SFU of the treated spheres compared to the control ones. The data are derived from the mean of duplicate wells of three independent experiments.

2.7. Statistical Analysis

The means ± the standard error of the means (SEM) of all independent repeats were calculated and the statistical analysis was performed using GraphPad Prism 9 Software (version 9.5.1, GraphPad Software Inc., La Jolla, CA, USA). A two-way ANOVA test was used to analyze the results of the MTT, trypan blue and wound healing assays, whereas a one-way ANOVA test was performed for the analysis of the

sphere-formation assay. Statistical significance was reported at p-values of < 0.05 . * $P < 0.05$; ** $P < 0.01$; *** $P < 0.001$.

CHAPTER 3

RESULTS

3.1. ONC201 and ONC206 Imipridones Decreased the Proliferation of DU145 and PC3 cells

We assessed the cytotoxic effect of ONC201 and ONC206 imipridones on the proliferation of the two PC cell lines DU145 and PC3 over three time points (24, 48 and 72 hours) using the MTT assay. Both cell lines were treated with increasing concentration of ONC201 and ONC206 ranging from 0.1 μM up to 10 μM . Treatment with both ONC201 and ONC206 led to a significant decrease in cellular proliferation in both cell lines in a time- and dose-dependent manner. Interestingly, cellular proliferation was significantly reduced with 5 μM ONC201 at 24h, 48h, and 72h post-treatment, whereas a 10-folds more potent anti-proliferative effect was detected with 0.5 μM ONC206 at the three time points post-treatment. No significant cytotoxic effect was observed with the vehicle (DMSO) (Figure 11).

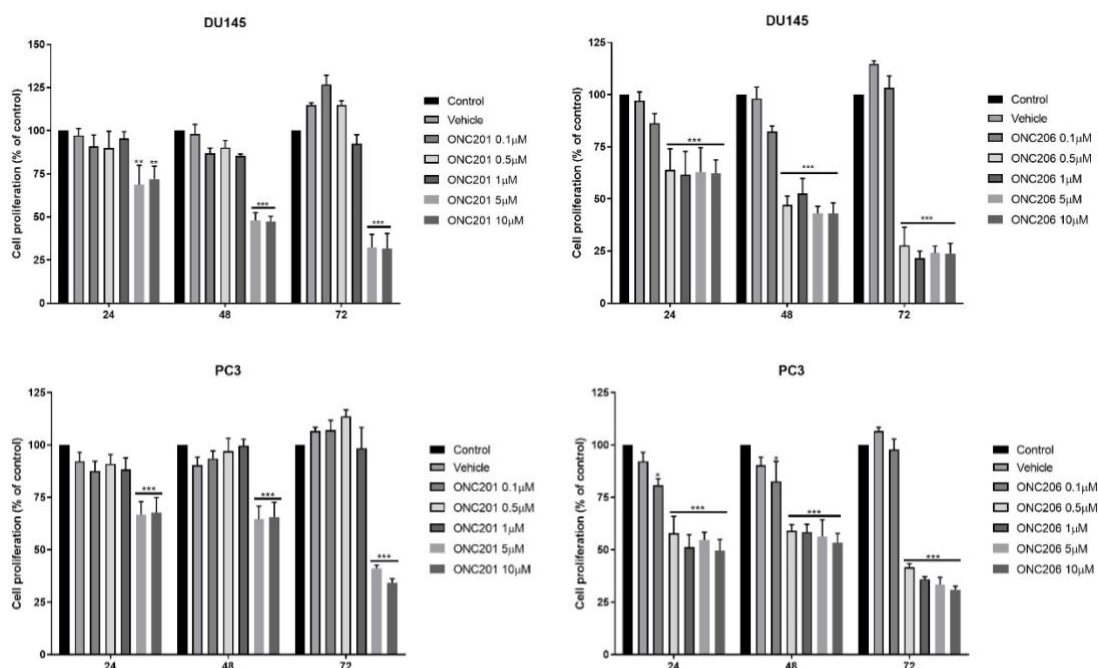


Figure 11. ONC201 and ONC206 decrease the proliferation of DU145 and PC3 cell lines in a time and dose-dependent manner. The anti-cancer effect of different concentrations of ONC201 and ONC206 on the proliferation of PC cells using MTT assay was determined in triplicates at 24, 48 and 72 h. Results are expressed as percentage of proliferation of the treated group compared to control at every time point. Data represent the mean \pm SEM of three independent experiments and are analyzed using two-way ANOVA (*P < 0.05; **P < 0.01; ***P < 0.001).

3.2. ONC201 and ONC206 Imipridones Reduced the Viability of DU145 and PC3 cells

As treatment with ONC201 and ONC206 revealed to decrease cellular proliferation, we tested the effect of both imipridones on the cells' viability using the trypan blue exclusion assay. DU145 and PC3 cell lines were treated with increasing concentrations of ONC201 and ONC206 varying from 0.5 μ M to 5 μ M. The results of the trypan blue method were consistent with the ones of the MTT assay. Our data showed that both drugs significantly reduced the viability of PC cells in a time- and dose-dependent manner with ONC206 exhibiting more potent effects (Figure 12). The counting results were supported by visually distinguishable morphological differences

between the treated and control groups. The DMSO vehicle did not show any effect on cellular viability.

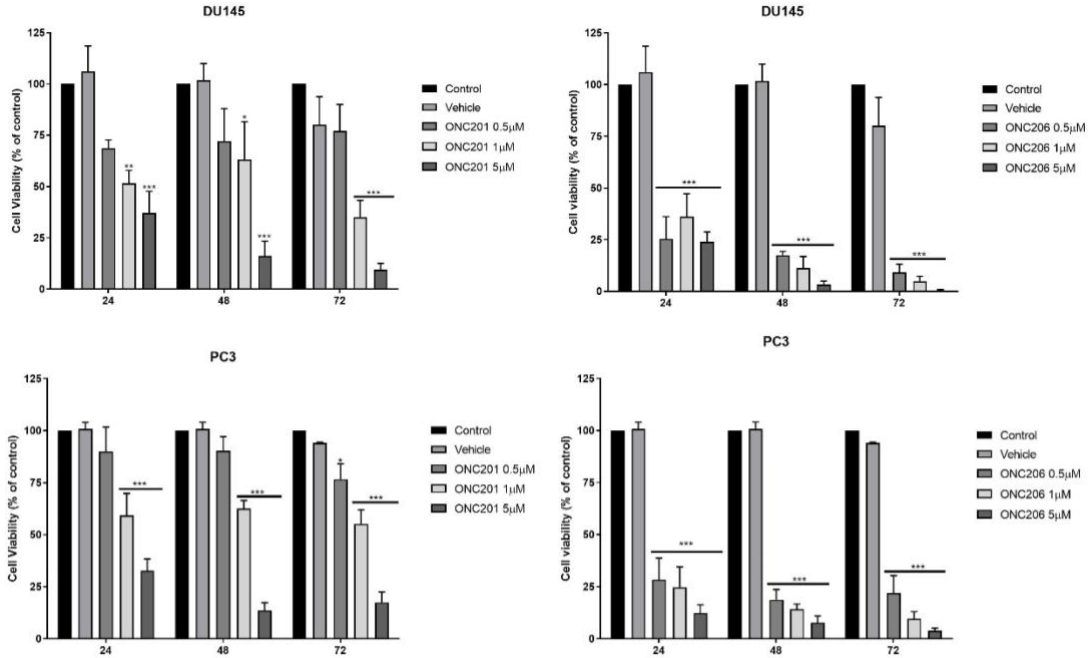


Figure 12. ONC201 and ONC206 reduce the viability of DU145 and PC3 cell lines in a time and dose-dependent manner. The anti-cancer effect of different concentrations of ONC201 and ONC206 on the viability of PC cells using trypan blue exclusion assay was determined in triplicates at 24, 48 and 72 h. Results are expressed as percentage of viability of the treated group compared to control at every time point. Data represent the mean \pm SEM of three independent experiments and are analyzed using two-way ANOVA (*P < 0.05; **P < 0.01; ***P < 0.001).

3.3. ONC201 and ONC206 Imipridones Attenuated the Migration of DU145 and PC3 cells

As migration is a crucial hallmark of cancer progression and metastasis, we investigated the ability of ONC201 and ONC206 imipridones in altering the migratory potential of DU145 and PC3 cell lines. For this purpose, we performed the wound healing or scratch assay. Our results indicated that the treatment of both cell lines with 5 μ M ONC201 and 0.5 μ M ONC206 significantly reduced the migratory ability of the cells as compared to the control and vehicle. The treated groups failed to close the

wound by more than 50% after 48h, contrary to the control groups that achieved complete wound closure upon the same time point (Figures 13 and 14).

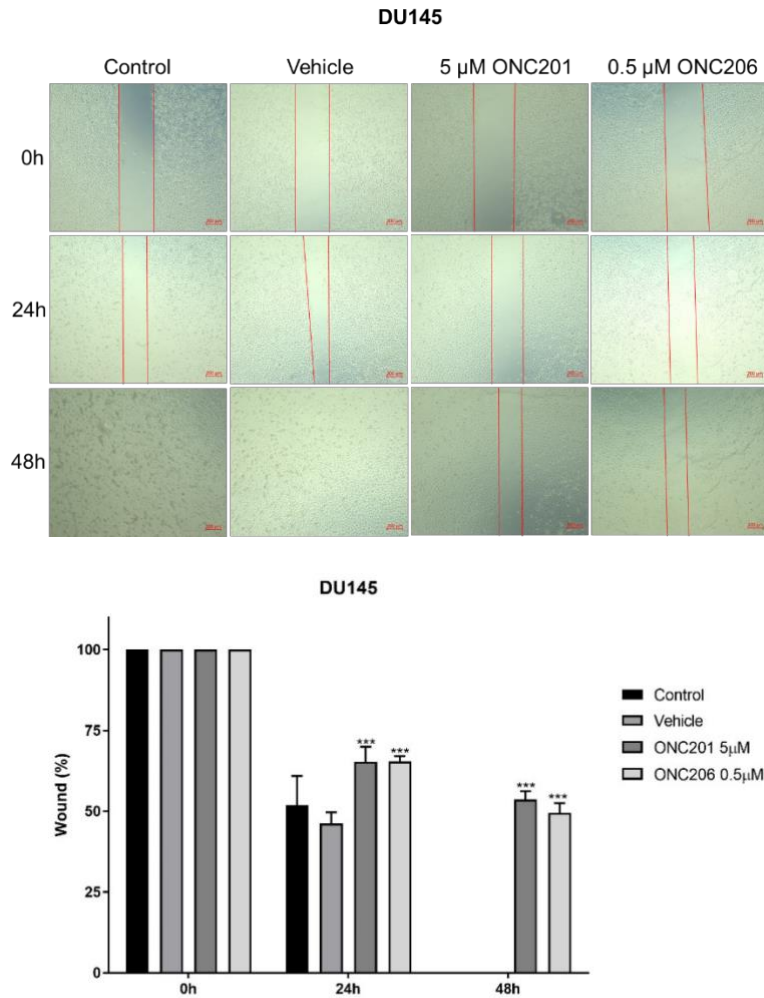


Figure 13. ONC201 and ONC206 attenuate the migration of DU145 prostate cancer cells. DU145 cells were seeded in 24-wells plate. A scratch was made on confluent cells using a 200 μ L tip and images were taken at 0, 24 and 48 h with or without the indicated treatment concentration. Representative images of wound healing assay at 5 \times magnification were taken (scale bar = 100 μ m). Quantification of the distance of the wound closure was assessed over time. Results are expressed as a percentage of each group compared to its condition at 0 h. Data represent the mean \pm SEM of three independent experiments and are analyzed using two-way ANOVA (*P < 0.05; **P < 0.01; ***P < 0.001).

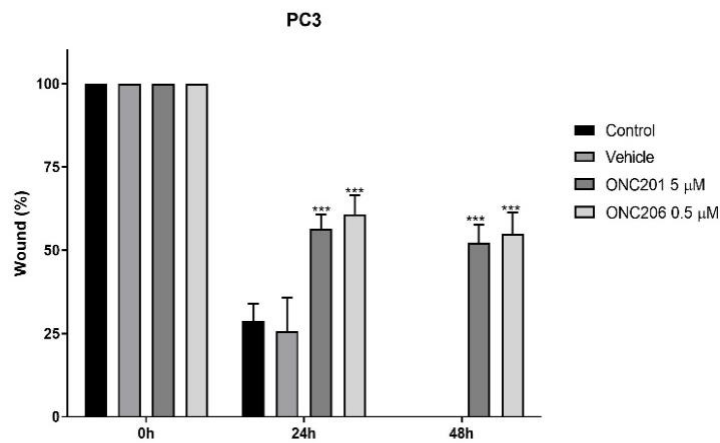
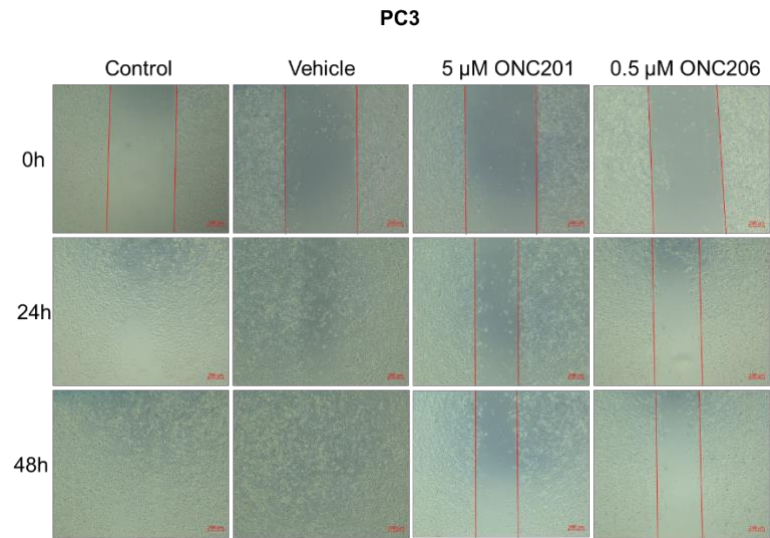


Figure 14. ONC201 and ONC206 attenuate the migration of PC3 prostate cancer cells. PC3 cells were seeded in 24-wells plate. A scratch was made on confluent cells using a 200 μ L tip and images were taken at 0, 24 and 48 h with or without the indicated treatment concentration. Representative images of wound healing assay at 5 \times magnification were taken (scale bar = 100 μ m). Quantification of the distance of the wound closure was assessed over time. Results are expressed as a percentage of each group compared to its condition at 0 h. Data represent the mean \pm SEM of three independent experiments and are analyzed using two-way ANOVA (* P < 0.05; ** P < 0.01; *** P < 0.001).

3.4. ONC201 and ONC206 Imipridones Decreased the Growth of DU145 and PC3 Cell-Derived Spheres

The ability of CSCs to grow as non-adherent spheroids in sphere medium has been widely used to assess their self-renewal capability. To check the potential of ONC201 and ONC206 imipridones in targeting the stem/progenitor cells within PC, the

sphere-forming assay was performed. DU145 and PC3 cells were cultured as single cells in Matrigel™ for 10-14 days and treated with ONC201 and ONC206. The spheres were then visualized under an inverted light microscope and bright-field images were taken (Figures 15 and 16). Our data showed that both cell lines formed spheres suggesting the presence of a unique subpopulation with stem cell-like properties. Notably, a dose-dependent attenuation of the SFU and size of DU145- and PC3-derived spheres was observed when treated with different concentrations of ONC201 (0.1, 0.5, 1, 2.5 μ M), and ONC206 (0.01, 0.1, 0.2, 0.5 μ M) (figure not shown). The SFU and spheres' size significantly decreased by more than half with 0.5 μ M ONC201 and 0.1 μ M ONC206 (Figures 15 and 16). Subsequently higher concentrations led to complete spheres eradication. These results indicate that ONC206 exerts a more potent effect than ONC201 in targeting the PCSCs subpopulation.

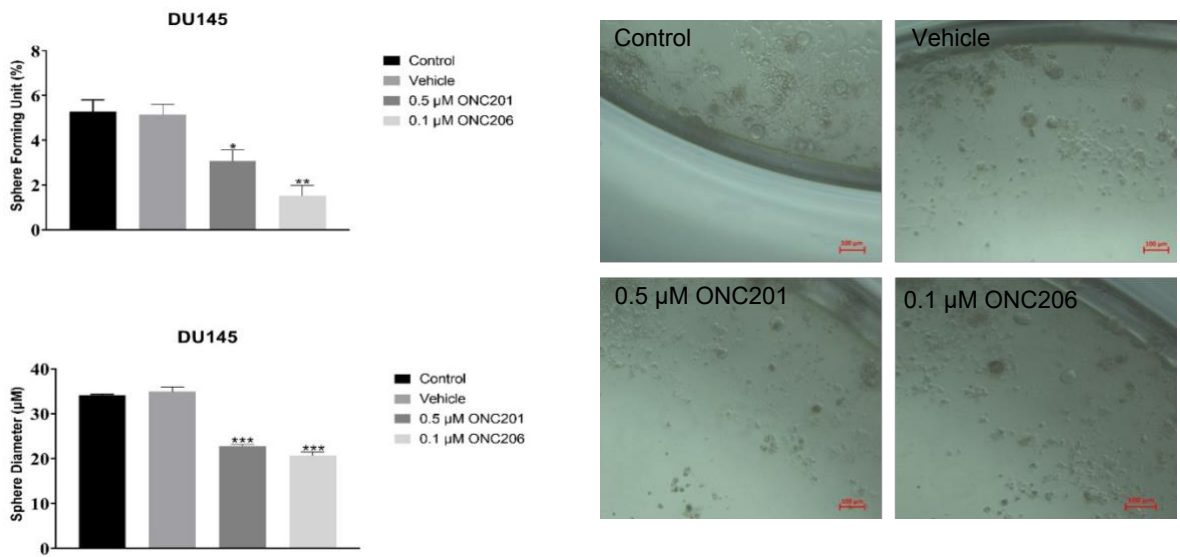


Figure 15. ONC201 and ONC206 decrease the sphere-forming unit and size of DU145-derived spheres. DU145 cells were seeded in duplicates at a density of 1,000 single cells/well in Matrigel™ for 10-14 days with and without treatment. Media or treatment was replenished every other day. Spheres were counted at day 10-14 of sphere culture. Results are expressed as SFU which is calculated according to the following formula: $SFU = (\text{number of spheres counted} / \text{number of input cells}) \times 100$. Spheres sizes were measured by Carl Zeiss Zen 2012 image software. Data represent an average diameter (µm) of 30 measured spheres. Representative bright field images of DU145 prostatospheres in Matrigel™ taken by the Axiovert inverted microscope are shown. Data represent the mean ± SEM of three independent experiments and are analyzed using one-way ANOVA (*P < 0.05; **P < 0.01; ***P < 0.001; treatment compared with control).

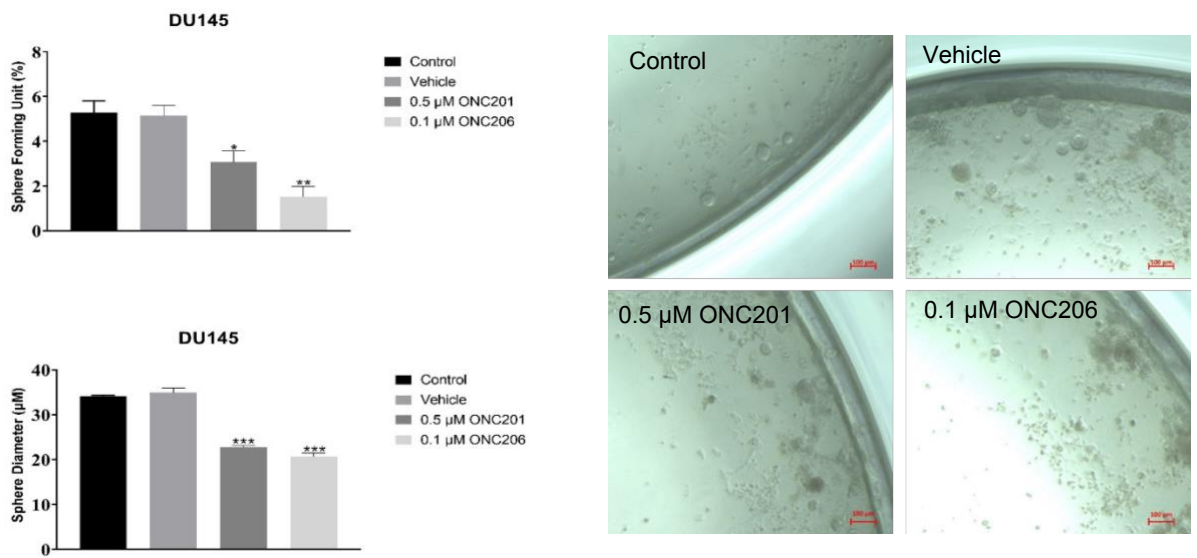


Figure 16. ONC201 and ONC206 decrease the sphere-forming unit and size of PC3-derived spheres. PC-3 cells were seeded in duplicates at a density of 1,000 single cells/well in Matrigel™ for 10-14 days with and without treatment. Media or treatment was replenished every other day. Spheres were counted at day 10-14 of sphere culture. Results are expressed as SFU which is calculated according to the following formula: $SFU = (\text{number of spheres counted} / \text{number of input cells}) \times 100$. Spheres sizes were measured by Carl Zeiss Zen 2012 image software. Data represent an average diameter (µm) of 30 measured spheres. Representative bright field images of PC3 prostatespheres in Matrigel™ taken by the Axiovert inverted microscope are shown. Data represent the mean ± SEM of three independent experiments and are analyzed using one-way ANOVA (*P < 0.05; **P < 0.01; ***P < 0.001; treatment compared with control).

CHAPTER 4

DISCUSSION

PC is the second most commonly diagnosed malignancy and the fifth leading cause of cancer related deaths in men worldwide [2]. This disease is considered a model for intra/inter-tumor heterogeneity, which constitutes a major hurdle that renders the effectiveness of the currently used therapeutic approaches [24]. PC progresses from an androgen-dependent stage that is responsive to ADT into an androgen-independent phenotype that resists conventional treatments [91]. Therefore, managing PC requires elucidating novel treatment strategies that can potentially overcome therapy resistance mechanisms. The CSCs subpopulation is believed to be a key driver of tumor initiation, progression, cancer relapse, and conventional therapy resistance [31]. Thus, the identification of novel therapeutics that can potentially eradicate PCSCs is primordial for the effective management of PC.

Imipridones are a novel family of anti-cancer compounds that can induce apoptosis of cancer cells while sparing the normal ones. Imipridones appear to operate under four main pathways [67]. They are TRAIL inducers that can activate apoptosis by binding to DR4 and DR5. Moreover, they can activate ISR that ultimately leads to cancer cell death. They were also shown to selectively antagonize DRD2, thus inhibiting cellular proliferation. Importantly, they can upregulate the degradation of proteins crucial to cancer cells survival by agonizing the mitochondrial protease ClpP [68, 92]. ONC201, the first in class-clinical imipridone, has shown promising results and has reached phase I/II clinical trials in several cancers including PC [67]. ONC201 was found to have anti-cancer effects in castration-sensitive and castration-resistant PC.

Indeed, it was able to target the AR signaling pathway resulting in the reduction of PSA levels. It also decreased the expression of AR splice variants 7(Arv-7), a cell surface marker expressed on PC cells resistant to ADT [80]. Hence, a more potent analog, ONC206, was derived to achieve significantly better results with less cytotoxicity to normal cells and prolonged efficacy compared to ONC201 [93]. However, there are currently no published studies assessing the anti-cancer effects of ONC206 on PC.

Our study was designed to investigate the anti-cancer potential of the novel therapeutic ONC206, in comparison to ONC201 in 2D and 3D culture models of PC. To our knowledge, this is the first study that tested the effects of ONC206 on the proliferation, viability and migration of PC cell lines. Importantly, this study assessed the ability of both imipridones in targeting the enriched subpopulation of PCSCs.

We first examined the cytotoxic effects of both imipridones at the 2D level on two human PC cell lines. Our results showed that ONC201 and ONC206 significantly decreased the proliferation and viability of both cell lines in a time- and dose-dependent manner. Moreover, both imipridones significantly attenuated the migratory potential of PC cells, which is a main hallmark of cancer. Collectively, our 2D data indicate that ONC201 and ONC 206 exert significant anti-neoplastic effects on PC cells.

Interestingly, ONC206 showed enhanced anti-tumor activity with 10-times more potent effect compared to ONC201. Indeed, a concentration of 0.5 μM ONC206 was able to achieve the same results as with 5 μM ONC201 at the proliferation, viability, and migration levels. Importantly, both imipridones led to a significant decrease in the size and sphere-forming ability of both PC cell lines, with a complete eradication of prostatospheres seen at high concentrations. Interestingly, a five-fold more potent effect was observed with ONC206, where 0.1 μM concentration was able to significantly

decrease the SFU and size of prostatospheres. However, a concentration of 0.5 μM of ONC201 was needed to reach the same outcome. These results implicate that both imipridones can target the subpopulation of PCSCs, thus overcoming one aspect of therapy resistance.

Our obtained results are consistent with previous findings that evidenced the enhanced potency of ONC206 in comparison with ONC201. ONC206 tested on human ovarian cancer cells showed a 10-fold reduction in the IC_{50} as compared to ONC201 [94]. Another study showed similar results in serous endometrial cancer, where ONC206 was shown to act under the same mode of action as ONC201 at nanomolar concentrations [86]. Moreover, El-Soussi *et al.* showed that both imipridones significantly decreased the proliferation, viability, migration, and invasion of neuroblastoma cell lines. Yet, ONC206 was able to induce apoptosis with a 10-times lower dose than that of ONC201. Additionally, the effect of ONC206 in decreasing the SFU and size of neuroblastoma spheres was five-fold greater than that of ONC201, which also correlates with our findings [88]. A study conducted in our laboratory by Monzer *et al.* investigated the differential anti-cancer potential between ONC201 and ONC206 on colorectal cancer cells. The results indicated that ONC206 exhibits more potent anti-cancer activity against colorectal cancer cell lines at the 2D level. Furthermore, the sphere formation assay revealed that ONC206 is 10-times more potent than ONC201 in inhibiting the self-renewal ability of colonospheres. Interestingly, this study assessed the effects of ONC201 and ONC206 in targeting CSCs using the patient-derived organoids model. ONC206 was shown to be more potent than ONC201 in inhibiting the growth of organoids' growth in three different patients, implicating its enhanced potency in targeting the CSCs subpopulation residing within the patient's

tumors [89]. Taken altogether, the anti-cancer potential of ONC206 against several cancer types is greater than that of ONC201 at the 2D and 3D levels.

Based on the promising anti-neoplastic effects of ONC201 on PC *in vitro* [67] as well as in phase I clinical trials [85], we sought to assess the effects of its analog derivative, ONC206, on two aggressive PC cell lines. Our data validated the greater efficacy of ONC206, in comparison with ONC201, at nanomolar doses in 2D and 3D culture systems. Nevertheless, the results need to be further confirmed by using additional cell lines that represent different stages of PC disease. Other bio-functional assays including trans-well invasion assay, cell cycle analysis, and reactive oxygen species (ROS) production assays should also be performed to study the anti-tumor effects of the drugs on other cancer hallmarks. Moreover, molecular assays should be used to assess the expression profile of markers associated with resistance mechanisms after treatment with both drugs. *In vivo* studies can also be employed to validate the results of the *in vitro* assays. Importantly, ONC206 will be tested in 3D PC patient-derived organoids model, a more reliable pre-clinical cancer model that mimics the genetics, histological and physiological characteristics of PC patients' tumor tissues.

In conclusion, our study demonstrated for the first time that ONC206 exhibits anti-cancer effects at nanomolar concentrations against PC, and is therefore more potent than ONC201. Our results strongly support the implication of the novel therapeutics ONC201 and ONC206 in the treatment of PC patients, paving the way for their promising clinical potential in PC patients that experience resistance to conventional therapies.

REFERENCES

1. Hanahan, D., *Hallmarks of Cancer: New Dimensions*. *Cancer Discov*, 2022. **12**(1): p. 31-46.
2. Sung, H., et al., *Global cancer statistics 2020: GLOBOCAN estimates of incidence and mortality worldwide for 36 cancers in 185 countries*. *CA: a cancer journal for clinicians*, 2021. **71**(3): p. 209-249.
3. Lakkis, N.A. and M.H. Osman, *Prostate Cancer in Lebanon: Incidence, Temporal Trends, and Comparison to Countries From Different Regions in the World*. *Cancer Control*, 2021. **28**: p. 10732748211055267.
4. Berenguer, C.V., et al., *Underlying Features of Prostate Cancer-Statistics, Risk Factors, and Emerging Methods for Its Diagnosis*. *Curr Oncol*, 2023. **30**(2): p. 2300-2321.
5. Cox, A., M. Jefferies, and R. Persad, *Prostate Structure and Function*. *Blandy's Urology*, 2019: p. 509-521.
6. Verze, P., T. Cai, and S. Lorenzetti, *The role of the prostate in male fertility, health and disease*. *Nat Rev Urol*, 2016. **13**(7): p. 379-86.
7. Anamthathmakula, P. and W. Winuthayanon, *Mechanism of semen liquefaction and its potential for a novel non-hormonal contraception†*. *Biol Reprod*, 2020. **103**(2): p. 411-426.
8. Coakley, F.V. and H. Hricak, *Radiologic anatomy of the prostate gland: a clinical approach*. *Radiol Clin North Am*, 2000. **38**(1): p. 15-30.
9. Singh, O. and S.R. Bolla, *Anatomy, abdomen and pelvis, prostate*. 2019.
10. McNeal, J.E., *The zonal anatomy of the prostate*. *Prostate*, 1981. **2**(1): p. 35-49.
11. De Marzo, A.M., et al., *Inflammation in prostate carcinogenesis*. *Nat Rev Cancer*, 2007. **7**(4): p. 256-69.
12. Barron, D.A. and D.R. Rowley, *The reactive stroma microenvironment and prostate cancer progression*. *Endocr Relat Cancer*, 2012. **19**(6): p. R187-204.
13. Vickman, R.E., et al., *The role of the androgen receptor in prostate development and benign prostatic hyperplasia: A review*. *Asian J Urol*, 2020. **7**(3): p. 191-202.
14. Butler, W. and J. Huang, *Neuroendocrine cells of the prostate: Histology, biological functions, and molecular mechanisms*. *Precision clinical medicine*, 2021. **4**(1): p. 25-34.
15. Huang, J., et al., *Immunohistochemical characterization of neuroendocrine cells in prostate cancer*. *The Prostate*, 2006. **66**(13): p. 1399-1406.
16. di Sant'Agnese, P.A., *Neuroendocrine cells of the prostate and neuroendocrine differentiation in prostatic carcinoma: a review of morphologic aspects*. *Urology*, 1998. **51**(5A Suppl): p. 121-4.
17. Collins, A.T., et al., *Identification and isolation of human prostate epithelial stem cells based on alpha(2)beta(1)-integrin expression*. *J Cell Sci*, 2001. **114**(Pt 21): p. 3865-72.
18. Toivanen, R. and M.M. Shen, *Prostate organogenesis: tissue induction, hormonal regulation and cell type specification*. *Development*, 2017. **144**(8): p. 1382-1398.
19. Taylor, R.A., et al., *Human epithelial basal cells are cells of origin of prostate cancer, independent of CD133 status*. *Stem Cells*, 2012. **30**(6): p. 1087-96.

20. Chen, X., et al., *New insights into prostate cancer stem cells*. Cell cycle, 2013. **12**(4): p. 579-586.
21. Walensky, L.D., et al., *A novel M(r) 32,000 nuclear phosphoprotein is selectively expressed in cells competent for self-renewal*. Cancer Res, 1993. **53**(19): p. 4720-6.
22. Bonkhoff, H. and K. Remberger, *Differentiation pathways and histogenetic aspects of normal and abnormal prostatic growth: a stem cell model*. Prostate, 1996. **28**(2): p. 98-106.
23. Easwaran, H., H.C. Tsai, and S.B. Baylin, *Cancer epigenetics: tumor heterogeneity, plasticity of stem-like states, and drug resistance*. Mol Cell, 2014. **54**(5): p. 716-27.
24. Haffner, M.C., et al., *Genomic and phenotypic heterogeneity in prostate cancer*. Nat Rev Urol, 2021. **18**(2): p. 79-92.
25. Li, J.J. and M.M. Shen, *Prostate Stem Cells and Cancer Stem Cells*. Cold Spring Harb Perspect Med, 2019. **9**(6).
26. Lawson, D.A., et al., *Basal epithelial stem cells are efficient targets for prostate cancer initiation*. Proc Natl Acad Sci U S A, 2010. **107**(6): p. 2610-5.
27. Wang, X., et al., *A luminal epithelial stem cell that is a cell of origin for prostate cancer*. Nature, 2009. **461**(7263): p. 495-500.
28. Reya, T., et al., *Stem cells, cancer, and cancer stem cells*. Nature, 2001. **414**(6859): p. 105-11.
29. Visvader, J.E. and G.J. Lindeman, *Cancer stem cells in solid tumours: accumulating evidence and unresolved questions*. Nat Rev Cancer, 2008. **8**(10): p. 755-68.
30. Aponte, P.M. and A. Caicedo, *Stemness in Cancer: Stem Cells, Cancer Stem Cells, and Their Microenvironment*. Stem Cells Int, 2017. **2017**: p. 5619472.
31. Huang, T., et al., *Stem cell programs in cancer initiation, progression, and therapy resistance*. Theranostics, 2020. **10**(19): p. 8721-8743.
32. Yin, W., et al., *Cancer and stem cells*. Exp Biol Med (Maywood), 2021. **246**(16): p. 1791-1801.
33. Espinosa-Sánchez, A., et al., *Therapeutic Targeting of Signaling Pathways Related to Cancer Stemness*. Front Oncol, 2020. **10**: p. 1533.
34. Chang, J.T. and S.A. Mani, *Sheep, wolf, or werewolf: cancer stem cells and the epithelial-to-mesenchymal transition*. Cancer Lett, 2013. **341**(1): p. 16-23.
35. Collins, A.T., et al., *Prospective identification of tumorigenic prostate cancer stem cells*. Cancer Res, 2005. **65**(23): p. 10946-51.
36. Gu, G., et al., *Prostate cancer cells with stem cell characteristics reconstitute the original human tumor in vivo*. Cancer Res, 2007. **67**(10): p. 4807-15.
37. Yehya, A., et al., *Tissue-specific cancer stem/progenitor cells: Therapeutic implications*. World J Stem Cells, 2023. **15**(5): p. 323-341.
38. Wang, L., et al., *Enrichment of prostate cancer stem-like cells from human prostate cancer cell lines by culture in serum-free medium and chemoradiotherapy*. Int J Biol Sci, 2013. **9**(5): p. 472-9.
39. Chang, L., et al., *Acquisition of epithelial-mesenchymal transition and cancer stem cell phenotypes is associated with activation of the PI3K/Akt/mTOR pathway in prostate cancer radioresistance*. Cell Death Dis, 2013. **4**(10): p. e875.

40. Castillo, V., et al., *Functional characteristics of cancer stem cells and their role in drug resistance of prostate cancer*. Int J Oncol, 2014. **45**(3): p. 985-94.
41. Germann, M., et al., *Stem-like cells with luminal progenitor phenotype survive castration in human prostate cancer*. Stem Cells, 2012. **30**(6): p. 1076-86.
42. Rybak, A.P., R.G. Bristow, and A. Kapoor, *Prostate cancer stem cells: deciphering the origins and pathways involved in prostate tumorigenesis and aggression*. Oncotarget, 2015. **6**(4): p. 1900-19.
43. Qin, J., et al., *The PSA(-/lo) prostate cancer cell population harbors self-renewing long-term tumor-propagating cells that resist castration*. Cell Stem Cell, 2012. **10**(5): p. 556-69.
44. Morrissey, C., et al., *Differential expression of angiogenesis associated genes in prostate cancer bone, liver and lymph node metastases*. Clin Exp Metastasis, 2008. **25**(4): p. 377-88.
45. Schatten, H., *Brief Overview of Prostate Cancer Statistics, Grading, Diagnosis and Treatment Strategies*. Adv Exp Med Biol, 2018. **1095**: p. 1-14.
46. Amin, M.B., et al., *The Eighth Edition AJCC Cancer Staging Manual: Continuing to build a bridge from a population-based to a more "personalized" approach to cancer staging*. CA Cancer J Clin, 2017. **67**(2): p. 93-99.
47. Carter, H.B., et al., *Early detection of prostate cancer: AUA Guideline*. J Urol, 2013. **190**(2): p. 419-26.
48. Gümüş, B.H., et al., *Does asymptomatic inflammation increase PSA? A histopathological study comparing benign and malignant tissue biopsy specimens*. Int Urol Nephrol, 2004. **36**(4): p. 549-53.
49. Ilic, D., et al., *Prostate cancer screening with prostate-specific antigen (PSA) test: a systematic review and meta-analysis*. bmj, 2018. **362**.
50. Carlsson, S.V. and A.J. Vickers, *Screening for Prostate Cancer*. Med Clin North Am, 2020. **104**(6): p. 1051-1062.
51. Naji, L., et al., *Digital Rectal Examination for Prostate Cancer Screening in Primary Care: A Systematic Review and Meta-Analysis*. Ann Fam Med, 2018. **16**(2): p. 149-154.
52. Tan, G.H., et al., *Smarter screening for prostate cancer*. World J Urol, 2019. **37**(6): p. 991-999.
53. Leslie, S.W., et al., *Prostate Cancer*, in *StatPearls*. 2023, StatPearls Publishing Copyright © 2023, StatPearls Publishing LLC.: Treasure Island (FL).
54. Descotes, J.L., *Diagnosis of prostate cancer*. Asian J Urol, 2019. **6**(2): p. 129-136.
55. Romero-Otero, J., et al., *Active surveillance for prostate cancer*. Int J Urol, 2016. **23**(3): p. 211-8.
56. Costello, A.J., *Considering the role of radical prostatectomy in 21st century prostate cancer care*. Nat Rev Urol, 2020. **17**(3): p. 177-188.
57. Podder, T.K., E.T. Fredman, and R.J. Ellis, *Advances in Radiotherapy for Prostate Cancer Treatment*. Adv Exp Med Biol, 2018. **1096**: p. 31-47.
58. Brawley, S., R. Mohan, and C.D. Nein, *Localized Prostate Cancer: Treatment Options*. Am Fam Physician, 2018. **97**(12): p. 798-805.
59. Pinkawa, M., *External beam radiotherapy for prostate cancer*. Panminerva Med, 2010. **52**(3): p. 195-207.
60. Heinlein, C.A. and C. Chang, *Androgen receptor in prostate cancer*. Endocr Rev, 2004. **25**(2): p. 276-308.

61. Desai, K., J.M. McManus, and N. Sharifi, *Hormonal Therapy for Prostate Cancer*. *Endocr Rev*, 2021. **42**(3): p. 354-373.
62. Grenader, T., et al., *Diethylstilbestrol for the treatment of patients with castration-resistant prostate cancer: retrospective analysis of a single institution experience*. *Oncol Rep*, 2014. **31**(1): p. 428-34.
63. Mitsogiannis, I., et al., *Prostate cancer immunotherapy*. *Expert Opin Biol Ther*, 2022. **22**(5): p. 577-590.
64. Hurwitz, M., *Chemotherapy in Prostate Cancer*. *Curr Oncol Rep*, 2015. **17**(10): p. 44.
65. Tannock, I.F., et al., *Docetaxel plus prednisone or mitoxantrone plus prednisone for advanced prostate cancer*. *N Engl J Med*, 2004. **351**(15): p. 1502-12.
66. Nader, R., J. El Amm, and J.B. Aragon-Ching, *Role of chemotherapy in prostate cancer*. *Asian J Androl*, 2018. **20**(3): p. 221-229.
67. Prabhu, V.V., et al., *ONC201 and imipridones: Anti-cancer compounds with clinical efficacy*. *Neoplasia*, 2020. **22**(12): p. 725-744.
68. Allen, J.E., et al., *Discovery and clinical introduction of first-in-class imipridone ONC201*. *Oncotarget*, 2016. **7**(45): p. 74380-74392.
69. Allen, J.E., et al., *Dual inactivation of Akt and ERK by TIC10 signals Foxo3a nuclear translocation, TRAIL gene induction, and potent antitumor effects*. *Sci Transl Med*, 2013. **5**(171): p. 171ra17.
70. Allen, J.E., R.N. Crowder, and W.S. El-Deiry, *First-In-Class Small Molecule ONC201 Induces DR5 and Cell Death in Tumor but Not Normal Cells to Provide a Wide Therapeutic Index as an Anti-Cancer Agent*. *PLoS One*, 2015. **10**(11): p. e0143082.
71. Yang, J.Y., et al., *ERK promotes tumorigenesis by inhibiting FOXO3a via MDM2-mediated degradation*. *Nat Cell Biol*, 2008. **10**(2): p. 138-48.
72. Ait Ghezala, H., et al., *Translation termination efficiency modulates ATF4 response by regulating ATF4 mRNA translation at 5' short ORFs*. *Nucleic Acids Res*, 2012. **40**(19): p. 9557-70.
73. Yuan, X., et al., *ONC201 activates ER stress to inhibit the growth of triple-negative breast cancer cells*. *Oncotarget*, 2017. **8**(13): p. 21626-21638.
74. Kline, C.L., et al., *ONC201 kills solid tumor cells by triggering an integrated stress response dependent on ATF4 activation by specific eIF2 α kinases*. *Sci Signal*, 2016. **9**(415): p. ra18.
75. Madhukar, N.S., et al., *A Bayesian machine learning approach for drug target identification using diverse data types*. *Nat Commun*, 2019. **10**(1): p. 5221.
76. Marisetty, A.L., et al., *REST-DRD2 mechanism impacts glioblastoma stem cell-mediated tumorigenesis*. *Neuro Oncol*, 2019. **21**(6): p. 775-785.
77. Greer, Y.E., et al., *ONC201 kills breast cancer cells in vitro by targeting mitochondria*. *Oncotarget*, 2018. **9**(26): p. 18454.
78. Graves, P.R., et al., *Mitochondrial Protease ClpP is a Target for the Anticancer Compounds ONC201 and Related Analogues*. *ACS Chem Biol*, 2019. **14**(5): p. 1020-1029.
79. Yang, Y., et al., *Repositioning Dopamine D2 Receptor Agonist Bromocriptine to Enhance Docetaxel Chemotherapy and Treat Bone Metastatic Prostate Cancer*. *Mol Cancer Ther*, 2018. **17**(9): p. 1859-1870.

80. Lev, A., et al., *ONC201 targets AR and AR-V7 signaling, reduces PSA, and synergizes with everolimus in prostate cancer*. *Molecular Cancer Research*, 2018. **16**(5): p. 754-766.
81. Wang, J., et al., *Silencing the epigenetic silencer KDM4A for TRAIL and DR5 simultaneous induction and antitumor therapy*. *Cell Death Differ*, 2016. **23**(11): p. 1886-1896.
82. Amoroso, F., et al., *Modulating the unfolded protein response with ONC201 to impact on radiation response in prostate cancer cells*. *Sci Rep*, 2021. **11**(1): p. 4252.
83. Prabhu, V.V., et al., *Cancer stem cell-related gene expression as a potential biomarker of response for first-in-class imipridone ONC201 in solid tumors*. *PLoS One*, 2017. **12**(8): p. e0180541.
84. Stein, M.N., et al., *First-in-Human Clinical Trial of Oral ONC201 in Patients with Refractory Solid Tumors*. *Clin Cancer Res*, 2017. **23**(15): p. 4163-4169.
85. Stein, M.N., et al., *Safety and enhanced immunostimulatory activity of the DRD2 antagonist ONC201 in advanced solid tumor patients with weekly oral administration*. *Journal for immunotherapy of cancer*, 2019. **7**: p. 1-9.
86. Zhang, Y., et al., *ONC206, an Imipridone Derivative, Induces Cell Death Through Activation of the Integrated Stress Response in Serous Endometrial Cancer In Vitro*. *Front Oncol*, 2020. **10**: p. 577141.
87. Wagner, J., et al., *Preclinical evaluation of the imipridone family, analogs of clinical stage anti-cancer small molecule ONC201, reveals potent anti-cancer effects of ONC212*. *Cell Cycle*, 2017. **16**(19): p. 1790-1799.
88. El-Soussi, S., et al., *A Novel Therapeutic Mechanism of Imipridones ONC201/ONC206 in MYCN-Amplified Neuroblastoma Cells via Differential Expression of Tumorigenic Proteins*. *Front Pediatr*, 2021. **9**: p. 693145.
89. Monzer, A., *Investigating the Anticancer Potential of Novel Therapeutics Using 3D Model Systems of Colon Cancer*. 2022.
90. Bahmad, H.F., et al., *Sphere-formation assay: three-dimensional in vitro culturing of prostate cancer stem/progenitor sphere-forming cells*. *Frontiers in oncology*, 2018. **8**: p. 347.
91. Rebello, R.J., et al., *Prostate cancer*. *Nat Rev Dis Primers*, 2021. **7**(1): p. 9.
92. Anderson, P.M., et al., *Phase II Study of ONC201 in Neuroendocrine Tumors including Pheochromocytoma-Paraganglioma and Desmoplastic Small Round Cell Tumor*. *Clin Cancer Res*, 2022. **28**(9): p. 1773-1782.
93. Bonner, E.R., et al., *Mechanisms of imipridones in targeting mitochondrial metabolism in cancer cells*. *Neuro Oncol*, 2021. **23**(4): p. 542-556.
94. Tucker, K., et al., *ONC206 has anti-tumorigenic effects in human ovarian cancer cells and in a transgenic mouse model of high-grade serous ovarian cancer*. *Am J Cancer Res*, 2022. **12**(2): p. 521-536.